Proceedings of the 28th IEEE
EMBS Annual International Conference
New York City, USA, Aug 30-Sept 3, 2006

Modeling Hippocampal Nonlinear Dynamic Transformations with Principal Dynamic Modes

Spiros H. Courellis, Theodoros P. Zanos, Min Chi Hsiao, Robert E. Hampson, Sam A. Deadwyler, Vasilis Z. Marmarelis, Theodore W. Berger

***Abstract*—A new modeling approach of hippocmapal nonlinear dynamics is presented. It is based on Principal Dynamics Modes (PDMs) derived from the Volterra kernels quantifying the hippocampal transformations. The approach is illustrated using data obtained from acute hippocampal slice preparations and from behaving rats performs a memory task. The resulting PDM models are comparable in performance to the Volterra models and require significantly less representational and implementational overhead.**

I. Introduction

Modeling the nonlinear dynamic transformations performed by the various hippocampal subsystems using the Volterra modeling approach has been one of our key areas of research for the past several years (e.g., [1], [2], [9]). More recently, we have been able to introduce single-input and multi-input Volterra models of the hippocampal areas based on data obtained from acute hippocampal slice preparations (e.g.,[3], [4], [5], [6], [7]) and on data collected from behaving rats [e.g., [10]]. The complexity of these models increases as the number of kernels included in the model increases and the size (memory) of each kernel increases. Implementations of multi-input Volterra models with higher than second order kernels and long memory can become even more complex as the number of inputs, order of the model, and the memory of the kernel increase.

One approach to address the complexity introduced by the number and the size of the kernels involves the introduction of models based on Principal Dynamic Modes derived from the computed Volterra kernels. In this paper, we present this approach and we illustrate its implementation and its use with data from two distinct experimental paradigms: acute hippocampal slice preparations and behaving rats performing a memory task.

Manuscript received April 3, 2006. This work was supported by ERC (BMES), DARPA (HAND), NIH (NIBIB).

S. H. Courellis is with the Biomedical Engineering Department, Viterbi School of Engineering, University of Southern California, Los Angeles, CA 90089 USA (213-740-0340; fax: 213-740-0343; e-mail: shc@usc.edu).

T. P. Zanos is with the Biomedical Engineering Department, Viterbi School of Engineering, University of Southern California, Los Angeles, CA 90089 USA (e-mail: zanos@usc.edu).

M. C. Hsiao is with the Biomedical Engineering Department, Viterbi School of Engineering, University of Southern California, Los Angeles, CA 90089 USA (e-mail: mhsiao@usc.edu).

V. Z. Marmarelis is with the Biomedical Engineering Department, Viterbi School of Engineering, University of Southern California, Los Angeles, CA 90089 USA (e-mail: vzm@usc.edu).

T. W. Berger is with the Biomedical Engineering Department, Viterbi School of Engineering, University of Southern California, Los Angeles, CA 90089 USA (e-mail: berger@usc.edu).

R. E. Hampson is with the Department of Physiology and Pharmacology, Wake Forest University, Winston-Salem, NC 27157 USA, (e-mail: hampson@wfubmc.edu)

S. A. Deadwyler is with the Department of Physiology and Pharmacology, Wake Forest University, Winston-Salem, NC 27157 USA, (e-mail: sdeadwyl@wfubmc.edu)

II. Methodology

A. Modeling Framework

The foundation of the modeling framework we used for representing nonlinear dynamic transformations performed by the various hippocampal subsystems is formed by the Volterra modeling approach. For a system with a singe input *[s(n), n=0,1,2…,N]* and a single output *[r(n), n=0,1,2,…, N]* the Volterra model is expressed mathematically by the following equation:

$$r(n) = k_0 + \sum_{m=0}^{M-1} k_1(m)\, s(n-m) + \tag{1}$$
$$+ \sum_{m_1}\sum_{m_2} k_2(m_1, m_2)\, s(n-m_1)\, s(n-m_2) +$$
$$+ \sum_{m_1}\sum_{m_2}\sum_{m_3} k_3(m_1, m_2, m_3)\, s(n-m_1)\, s(n-m_2)\, s(n-m_3) +$$
$$+ \text{higher order terms}$$

where k_0 is the zeroth order kernel, k_1 is the first order kernel, k_2 is the second order kernel, k_3 is the third order kernel, and so on. The first order kernel captures the effect of past input values on the current output value and models the linear part of the system. Higher order kernels capture the effect on the output of interactions among κ-tuples of input values, where κ is the order of the kernel; i.e., second (κ=2), third (κ=3) and so on. Higher order kernels model the nonlinear part of the system.

Depending on the experimental paradigm and the assumptions made for the data analysis, the basic Volterra modeling approach has been adapted accordingly. Data from hippocampal slice preparations were obtained by employing Poisson distributed impulse sequences applied at perforant path. The CA3 hippocampal region was modeled using the amplitude of the evoked population spikes recorded at the dentate granule cell layer (input) and the corresponding population spikes at the CA3 pyramidal cell layer (output)[3]. Thus, modeling hippocampal nonlinear transformations using this type of data incurred reduction in kernel dimensionality ([7]). As a result, equation 1 was

reduced to:

$$r(n_i) = A_i k_1 + A_i \sum_{n_i-\mu<n_j<n_i} A_j k_2(n_i - n_j) + \quad (3)$$
$$+ A_i \sum_{n_i-\mu<n_{j1}<n_i} \sum_{n_i-\mu<n_{j2}<n_i} A_{j_1} A_{j_2} k_3(n_i - n_{j_1}, n_i - n_{j_2})$$

where A_i, A_j represent the varying amplitudes of the population spikes recorded at the input of the modeled hippocampal subsystem (e.g., the granule cell layer), $r(n_i)$ represents the amplitude of the population spikes recorded at the output of the modeled hippocampal subsystem (e.g., CA_3), k_1, k_2, and k_3 are the first, second, and third-order kernels respectively, n_i is the time of occurrence of the current impulse in the I/O sequence, and n_j is the time of occurrence of the jth impulse prior to the present impulse within the kernel's memory window μ.

Modeling hippocampal nonlinear dynamic transformations using experimental data from behaving rats was not subject to the same data analysis assumptions as the hippocampal slice case. Data from behaving rats were comprised of natural spike sequences recorded at the CA3 pyramidal cell layer (input) and the CA1 pyramidal cell layer (output)[10]. In this case, the exact causal relationship that existed in the case of the data from the hippocampal slice can not be asserted. Thus, equation (1) was used as the basis to represent this class of models. In this case, multi-input models were found to be necessary to increase the representation accuracy. An extension of the basic Volterra equation (eq. 1) for multiple inputs was introduced to satisfy this requirement. Since, both input and output were binary sequences of spikes, besides the kernels, the model included components that determine when a spike will be generated or not. The mathematical formalization of the model is as follows:

$$u(n) = k_0 + \sum_{m=0}^{M-1} k_{1s_q}(m)\, s(n-m) +$$
$$+ \sum_{m_1} \sum_{m_2} k_{2s_q s_q}(m_1, m_2)\, s_q(n-m_1)\, s_q(n-m_2) + \quad (2)$$
$$+ \sum_{m_1} \sum_{m_2} \sum_{m_3} k_{3s_q s_q s_q}(m_1, m_2, m_3)\, s_q(n-m_1)\, s_q(n-m_2)\, s_q(n-m_3)$$

$$v(n) = f(u)$$
$$r(n) = TT[v] = \begin{cases} 1 & if\ v > \theta \\ 0 & otherwise \end{cases}$$

where Q is the number of inputs $s_q(n)$, $r(n)$ is the output, $\{k_{0sq}, k_{1sq}, k_{2sq}, k_{3sq}\}$ represent the zero, first, second, and third order Volterra kernels for the corresponding inputs s_q, and $u(n)$ denotes the output of the kernel subsystem. $f(u)$ is a static nonlinear function that assigns a probability of firing $[v(n)]$ to each value of $u(n)$. The thresholding operator $[TT(v)]$ that follows partitions the *u-domain* in firing and non-firing areas and produces the final binary spike output $r(n)$.

B. Modeling with Principal Dynamic Modes

The expression of a Volterra model in terms of it principal dynamic modes has it roots in the Wiener-Bose model [ref] and the approximation of matrix-vector representation of equation (1) by approximating the matrix by its most significant eigenvectors [8]. Figure 1 shows an example of a single input / single output N-th order Volterra model (Fig. 1A) and its equivalent model based on principal dynamic modes (Fig. 1B).

The PDM model convolves the input $[s(n)]$ with each PDM $[\mu_p(n)]$ and feeds the result of each convolution $[u_p(n)]$

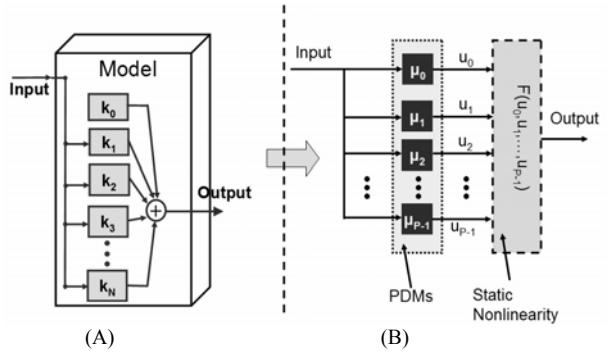

Fig. 1. An example of a single input / single output N-th order Volterra model (A) and its equivalent model based on principal dynamic modes (B).

to a static nonlinearity $[F(u_1, u_2, ..., u_P)]$, where P is the number of PDMs in the model. The output of this nonlinearity is the response of the PDM model.

One way to compute the principal dynamic modes is to compute the kernels first, then perform eigendecomposition of the matrix in a matrix-vector representation of equation 1, and consider the eigenvectors corresponding to the most significant eigenvalues as the principal dynamic modes (PDMs). $[F(u)]$ that is computed from the $\mathbf{u(n)}=(u_1(n), u_2(n), ..., u_P(n))^T$ vectors and the corresponding output values $r(n)$.

C. Reduction in Model Complexity

The Voletrra models we computed for hippocampal regions based on the slice preparation and the behaving rats included up to third order terms. In both cases, model representation based on kernels introduces implementational challenges in terms of space for storing the kernels and computational effort for calculating the "special convolutions" between the kernels and the input, especially when third order kernels are included.

The PDM based models are significantly simpler. Each mode requires as much storage as a first order kernel and generally a small number of modes is required, at least in our cases as it is illustrated by the results section. The static nonlinearity can be implemented either explicitly through a lookup table or through an approximation analytically or via an Artificial Neural Network.

III. Results

Volterra models and the corresponding PDM models were computed for one case involving data from behaving rats

and one case involving data from an acute hippocampal slice. In both cases, a third order single-input/single output model has been selected.

The Volterra kernels of the model for the CA3→CA1 transformation performed by the hippocampus of the behaving rat is shown in Fig. 2. Figure 2A shows the first order kernel, characterized by a depressive phase in the beginning that transitions to a slight facilitatory phase after crossing the zero-axis at about 100ms. The second order kernel (Fig. 2B) exhibits facilitatory behavior in the beginning that is succeeded by a shallow depressive phase before its returns to the zero-plane. The third order kernel is four-dimensional. Thus only slices can be shown. The slices of the third order kernel at 50msec (Fig. 2C) and 150msec (Fig. 2D) exhibit predominantly depressive behavior.

The firing probability function (Fig. 2E) has a main peak

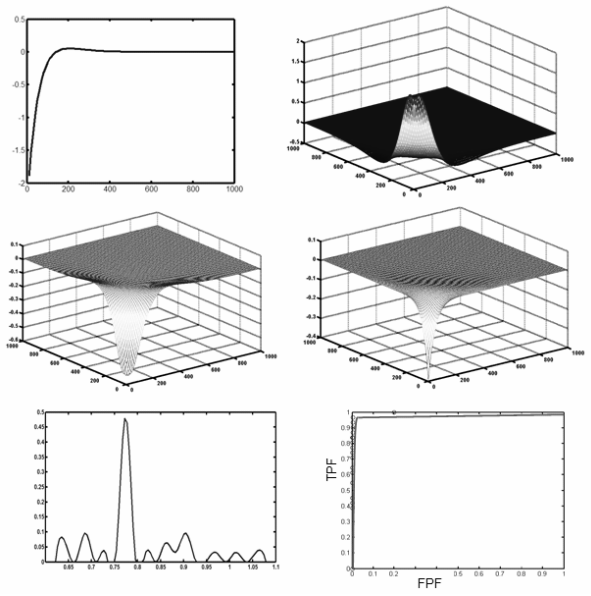

Fig. 2. Third order single input / single output model of the CA3→ CA1 functional mapping using data from behaving rats. First Order kernel (A), second order kernel (B), and third order kernel slices at 50msec (C) and at 150msec (D). Firing probability function (E), and ROC curve (F).

around u=0.775 and smaller peaks at different u-values. Around the peak the probability of firing is close to 50%. The predictive accuracy of the model was evaluated by the ROC curve shown in Figure 2F. The best true positive fraction (TPF) was close to 100% while the corresponding false positive fraction (FPF) was 0.8%. These values indicate that the model predicted almost 100% of the spikes and generated spikes erroneously (while they did not exist in the actual dataset) rarely.

The PDM model corresponding to the Volterra model of Fig. 2 is shown in Fig. 3. There were only three significant PDMs that are shown in Fig. 3A, 3B, and 3C. The first PDM (Fig. 3A) exhibits predominately depressive behavior with slight facilitation after 200msec. The second PDM (Fig. 3B) starts with a very fast facilitatory phase that quickly becomes depressive between about 40msec and 160msec. After, 160msec, it exhibits a slower facilitatory phase before it returns to the zero line. The third PDM starts with a fast facilitatory phase succeeded by a shallow depressive phase and an even shallower facilitatory phase. The static nonlinearity that succeeds the filter bank of the PDMs is four-dimensional and thus only slices can be shown. Fig. 3D, 3E, and 3F show slices of this function. Regions of firing are clearly defined with increasing probability from the slice in Fig. 3D (max probability = 0.3) to the slice in Fig. 3E (max probability = 0.8). The ROC curve in this case was comparable to the one in Fig. 2F.

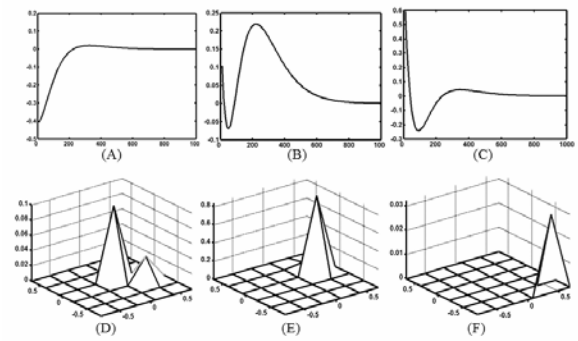

Fig. 6. PDM equivalent model for the Volterra model shown in Fig.5. First (A), second (B), and third (C) principal dynamic mode, and slices of the static nonlinearity that follows.

The prediction accuracy of both models was very high. Besides the values of the TPF and the FPF given by the ROC curves in both case, comparison between the actual response and the predicted response by each model confirm it. The data segment from the actual response of the CA1 neuron (Fig. 4A) compares very favorably with its counterpart predicted by the Volterra model (Fig. 4B) and by the PDM model (Fig. 4C).

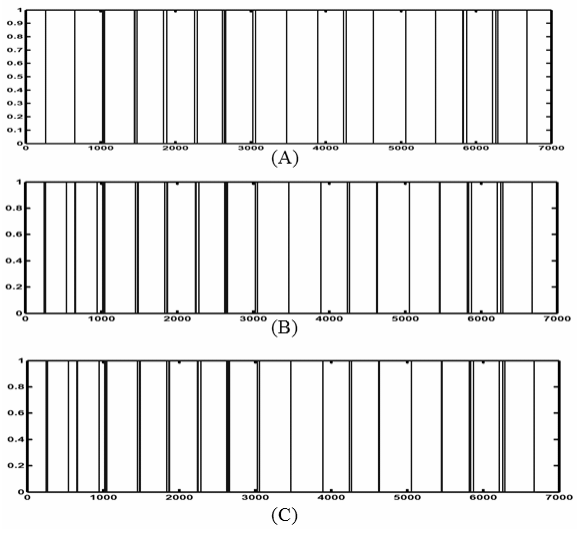

Fig. 4. Model responses shown in Fig. 2 and Fig. 3. Response of the Volterra model (B) and the PDM model (C) compared to the recorded response from CA1 (A).

The Volterra kernels of the model for the Dentate→CA3 transformation performed by the hippocampus of acute hippocampal slice is shown in Fig. 5. Figure 5A shows the second order kernel, exhibiting facilitatory behavior. The third order kernel (Fig. 5B) exhibits a very sharp depressive phase in the beginning followed by a shallow facilitatory phase (especially close to the axes) before it returns to the zero-plane. Note, that in the case of the slice preparation, the data analysis assumptions lead to dimensionality reduction for all the kernels by one dimension.

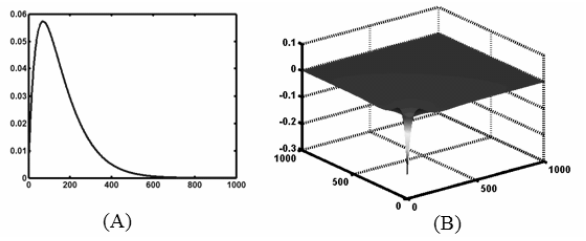

Fig. 5. Volterra-Poisson kernels using data from an acute hippocampal slice preparation: second order kernel (A) and third order kernel (B).

The PDM model corresponding to the Volterra model of Fig. 5 is shown in Fig. 6. Just like in the case involving data from the behaving rats, there were only three significant PDM that are shown in Fig. 6A, 6B, and 6C.

The first PDM (Fig. 6A) starts with a very fast facilitatory phase that quickly becomes depressive between about 50msec and 180msec. After, 180msec, it exhibits a slight facilitatory phase before it returns to the zero line. The second PDM (Fig. 6B) exhibits only depressive behavior. The third PDM starts with a fast facilitatory phase succeeded by a slower depressive phase. The static nonlinearity that succeeds the filter bank of the PDMs is four-dimensional and thus only slices can be shown. Fig. 6D, 6E, and 6F show slices of this function. Regions of firing and regions of non activity are clearly defined. A comparison between the

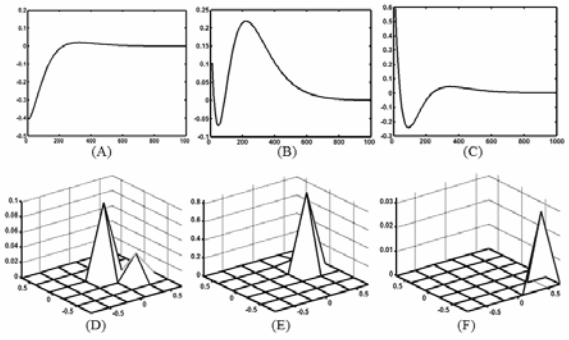

Fig. 6. PDM equivalent model for the Volterra model shown in Fig.5. First (A), second (B), and third (C) principal dynamic mode, and slices of the static nonlinearity that follows.

normalized mean square error computed between the recorded response and the prediction of Volterra model is close to the normalized mean square error computed between the recorded response and the prediction of the PDM model.

IV. Discussion

We introduced a new approach for modeling hippocampal nonlinear dynamic transformations. It is based on the Principal Dynamic Modes of the transformation computed from the kernels of its Volterra model. PDM models clearly provide a representation of considerably less complexity when it comes to storage and computational effort. For example consider the case of the single-input/single output model using the data from behaving rats. A third order Volterra model involving kernels with 1 sec. memory and resolution of 10 msec. would require storing about 170,000 floating point numbers for the kernels (after taking into account kernel symmetries). The corresponding PDM model included three PDMs with storage requirements of 300 floating point numbers and a static nonlinearity with storage requirements of 125 floating point numbers. The computational effort is significantly less intensive in the case of the PDM model, since the overwhelming triple convolutions of the third order kernels are absent. Similar conclusions can be drawn for the hippocampal slice case. These initial results are indicative of a trend that may extend when multiple inputs are involved. Thus, a more extensive study examining more cases in greater details is worthwhile.

References

[1] T. W. Berger, Eriksson J.L., Ciarolla D.A., and Sclabassi R.J. (1988): Nonlinear systems analysis of the hippocampal Perforant Path-Dentate projection. II Effects of random train stimulation : *J Neurophsiol.* 60:1077-1094.

[2] T. W. Berger, Eriksson J.L., Ciarolla D.A., and SclabassiR.J. (1988b): Nonlinear systems analysis of the hippocampal Perforant Path-Dentate projection. III Comparison of random train and paired impulse stimulation. *J Neurophsiol*. 60:1095-1109.

[3] T. W. Berger, A. Ahuja, S. H. Courellis et al, "Restoring lost cognitive function", *IEEE Engineering in Medicine and Biology Magazine*, vol. 24(5), pp. 30–44, Sept.-Oct. 2005.

[4] A. Dimoka, S.H. Courellis, D. Song, V.Z. Marmarelis, and T.W Berger. Identification of the Medial and the Lateral Perforant Path using Single and Dual Random Impulse Train Stimulation. *Proc. of IEEE-EMBS 2003.*

[5] S. H. Courellis, G. Gholmieh, V.Z. Marmarelis and T. W. Berger. Modeling Nonlinear Neural Dynamics with Volterra-Poisson Kernels. Proceedings*, 2004 IEEE International Joint Conference on Neural Networks,* Volume: 4, 25-29 July 2004, pp. 3219 – 3222.

[6] S. H. Courellis, Marmarelis, V.Z. and T.W. Berger. Modeling Event-Driven Nonlinear Dynamics in Biological Neural Networks*, Proc. of 7th Symposium on Neural Computation*, vol. 10, pp. 28-35, Los Angeles, CA.

[7] G. Gholmieh, S. H. Courellis, V. Z. Marmarelis and T.W. Berger, "An efficient method for studying short term plasticity with random impulse train stimuli", *Journal of Neuroscience Methods,* vol. 21(2), pp. 111-127, Dec. 2002.

[8] V. Z. Marmarelis, *Nonlinear Dynamic Modeling of Physiological Systems.* New York, NY: Wiley, 2004, ch. 2.

[9] Sclabassi R.J. , Eriksson J.L, Port R., Robinson G. and Berger T.W (1988): Nonlinear Systems Analysis of the Hippocampal Perforant Path-Dentate Projection I. Theoretical and Interpretational Considerations: *J Neurophysiol.* 60:1066-1076.

[10] T. P. Zanos, S. H. Courellis, R. E. Hampson, S. A. Deadwyler, V. Z. Marmarelis and T. W. Berger, " A multi-input modeling approach to quantify hippocampal nonlinear dynamic transformations " *Proc. of IEEE-EMBS 2006.*